NJC

PAPER

View Article Online
View Journal

Cite this: DOI: 10.1039/c7nj05039a

Rhodium(triphenylphosphine)carbonyl-2,4-dioxo-3-pentyl-4-decanyloxybenzoate: synthesis, electrochemistry and oxidative addition kinetics†

Nomampondomise F. Stuurman, Blenerhassitt E. Buitendach, Linette Twigge, Pieter J. Swarts and Jeanet Conradie *

The synthesis, electrochemistry and oxidative addition kinetics are presented for a new [Rh(β-diketonato)(CO)(PPh_3)] complex (**2**), of rhodium metal complexed with a β-diketonato ligand, β-L1 = $(CH_3COC(C_{10}H_{21}O\text{-}C_6H_4COO)COCH_3)^-$, containing a long and sterically large chain (R^α = $C_{10}H_{21}OC_6H_4COO$) substituted at the α position. This rhodium triphenylphosphine complex (**2**), [Rh(β-L1)(CO)(PPh_3)], was subsequently converted from a rhodium(I) to a rhodium(III) complex, by chemical and electrochemical oxidation. The kinetics of the chemical conversion from Rh^I to Rh^{III}, which was obtained by the oxidative addition reaction [Rh(β-L1)(CO)(PPh_3)] + CH_3I, demonstrated that the reaction occurs in two reaction steps, with a Rh^{III}-alkyl species as the main reaction product. The sterically large and long chain (R^α = $C_{10}H_{21}OC_6H_4COO$) at the α-position of the β-diketonato ligand, did not at all affect either the second order reaction rate constant (k_1) of the first oxidative addition step of the [Rh(β-L1)(CO)PPh_3] + CH_3I reaction, nor the value of the oxidation potential (E_{pa}) of the electrochemical oxidation of [Rh^I(β-L1)(CO)PPh_3] to a Rh^{III}-species. This was proven *via* a literature study, by comparing the k_1 and E_{pa} values from this study with the respective rate constants (k_1) and oxidation potentials (E_{pa}) of a wide variety of related [Rh(β-diketonato)(CO)(PPh_3)] complexes without such a R^α substituent at the α position.

Received 19th December 2017,
Accepted 6th February 2018

DOI: 10.1039/c7nj05039a

rsc.li/njc

1 Introduction

β-Diketones are 1,3-diketones bearing two carbonyl groups separated by one carbon atom, referred to as the α-carbon (Fig. 1). Many β-diketones, with different substituents on the 1 and 3 position and a hydrogen atom on the α-carbon are known,[1] the most well-known being acetyl acetone (Hacac) with methyl groups on both the 1 and 3 positions. Not many β-diketones are known with substituents on the α-carbon. The β-diketones exhibit keto–enol tautomerism (Fig. 1).[2] In solution, the enol form is often the dominant form, due to the stabilization of the intramolecular hydrogen bond. The H-atom of the alcohol group of the enol form can easily be removed to form a metal-β-diketonato complex, a property often used in the solvent extraction of metals.[3] Rhodium-β-diketonato complexes, such as the rhodium dicarbonyl [Rh(β-diketonato)$(CO)_2$][4–10] and rhodium triphenylphosphine [Rh(β-diketonato)(CO)(PPh_3)][11,12]

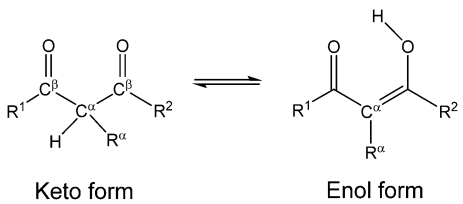

Fig. 1 Enol–keto tautomerism of β-diketones. For most β-diketones, substituent R^α = H, however in this study R^α = $C_{10}H_{21}OC_6H_4COO$, a long and sterically large group, substituted at the α-position.

complexes, are well-known. The first step of the oxidative addition reaction of methyl iodide to the latter complex,[13] is similar to the oxidative addition reaction step of methyl iodide to the rhodium(I) Monsanto catalyst, used during the process of manufacturing acetic acid by the catalytic carbonylation of methanol.[14]

The oxidative addition of methyl iodide to a variety of rhodium triphenylphosphine complexes [Rh(β-diketonato)(CO)(PPh_3)], has been studied for a series of different β-diketonato ligands,[15–18] all showing that the oxidative addition step is followed by a methyl migration step(s). Generally it was found that electron donating substituents R^1 and R^2 on the β-diketone ligand (Fig. 1) enhance the rate (higher second order rate constant k_1) of oxidative

Department of Chemistry, University of the Free State, PO Box 339, 9300 Bloemfontein, Republic of South Africa. E-mail: conradj@ufs.ac.za; Fax: +27-51-4017295; Tel: +27-51-4012194

† Electronic supplementary information (ESI) available: Fig. S1–S4 provide the structures of the complexes, as well as selected ^{31}P NMR spectra which were recorded during the oxidative addition reaction, [Rh(β-L1)(CO)PPh_3] + CH_3I. See DOI: 10.1039/c7nj05039a

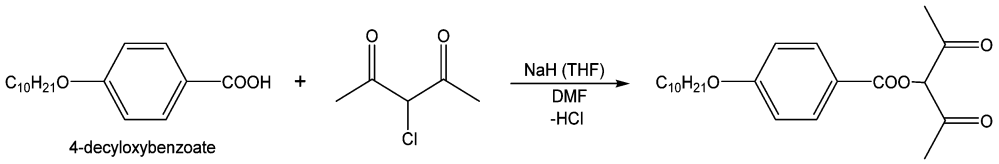

Scheme 1 Synthetic route for the synthesis of the long and sterically large α-substituted β-diketone ligand, namely: 2,4-dioxo-3-pentyl-4-decanyloxybenzoate ($CH_3COCH(C_{10}H_{21}OC_6H_4COO)COCH_3$), referred to as the Hβ-L1 ligand in this study.

addition,[19] while electron withdrawing substituents led to a slower oxidative addition rate.[20,21] However, a kinetic study of a specific complex, $[Rh((C_6H_5)COCHCOR^2)(CO)(PPh_3)] + CH_3I$ (with $R^2 = (CH_2)_nCH_3$, n = 1–3) where the substituent R^2 (Fig. 1) is an alkyl chain of increasing length, showed that the first oxidative addition step was not at all influenced by the increasing alkyl chain length of the R^2 group substituted on the β-diketonato ligand.[22] This was contrary to expectation, since steric factors generally influence the rate of oxidative addition reactions.[23,24] The objective of this work is to synthesize and characterize a [Rh(β-diketonato)(CO)(PPh_3)] complex with a β-diketonato ligand containing a long and sterically large chain on the α-position, and to investigate the influence of the long α-substituent on the rate of oxidative addition (k_1) of methyl iodide to this [Rh(β-diketonato)(CO)(PPh_3)] complex (**2**), as well as on the oxidation potential (E_{pa}) of the electrochemical oxidation of Rh^I to Rh^{III}, when compared to the same reaction of known rhodium triphenylphosphine complexes without such a α-substituent, as obtained from literature. The β-diketone chosen for this study is ligand ($CH_3COCH(C_{10}H_{21}OC_6H_4COO)COCH_3$), referred to as Hβ-L1, see Scheme 1 and Fig. 2.

2 Experimental

2.1 Materials and apparatus

Solid and liquid materials (Merck, Aldrich) were used without further purification. The solvents were distilled before use and water was doubly distilled. Flash chromatography was performed on Silica gel 60 (Merck, grain size 0.040–0.063 mm), utilizing an overpressure not exceeding 100 Torr (1 Torr = 1 mmHg = 133.32 Pa). Liquid reactants were distilled prior to use. Organic solvents were dried according to published methods.[25]

2.2 Synthesis

2.2.1 Synthesis of the Hβ-L1 ligand: 2,4-dioxo-3-pentyl 4-decanyloxybenzoate $CH_3COCH(C_{10}H_{21}OC_6H_4COO)COCH_3$, (Hβ-L1). The sodium salt of 4-decyloxybenzoate was synthesised by slowly adding 4-decyloxybenzoic acid (0.02 mol, 5.688 g) in THF (15 ml pre-dried overnight), to a stirred suspension of sodium hydride (0.02 mol, 0.480 g) in THF (20 ml pre-dried overnight). The reaction mixture was stirred overnight at room temperature. Anhydrous DMF (25 ml) was added to the product and stirred under argon for 30 minutes, followed by the addition of 3-chloropentane-2,4-dione (0.02 mol, 2.692 g) in 10 ml of anhydrous DMF. Argon was passed through the light orange reaction mixture for another 30 minutes, after which the reaction was stirred under reflux at 50–60 °C for 24 hours. A light yellow reaction mixture was obtained and cooled to room temperature. Water (200 ml) was added and the product was extracted twice with 50 ml $CHCl_3$. Extractions were dried over sodium sulfate and the solvent was evaporated under reduced pressure. The product was purified by column chromatography, with a hexane : ethylacetate (1 : 3) solution as eluant, and further purified by re-crystallisation in benzene. This resulted in a pale pink solid, with a yield of 4.8348 g (85%). M.p. 61.63 °C.

^{1}H NMR (600 MHz, $CDCl_3$, 25 °C, numbering of C is given in Fig. S1 in the ESI†): δ 14.50 (s, Enol-H), 8.05 (d, $^3J_{H-H}$ = 8.9 Hz, 3′- & 5′-H), 6.93 (d, $^3J_{H-H}$ = 8.9 Hz, 2′- & 6′-H), 5.70 (s, H), 4.02 (t, $^3J_{H-H}$ = 6.6 Hz, 1-CH_2), 2.39 (s, CH_3-β), 2.06 (s, CH_3-β), 1.81 (m, 2-CH_2), 1.46 (m, 3-CH_2), 1.40–1.20 (m, 4–9-CH_2), 0.88 (t, $^3J_{H-H}$ = 6.9 Hz, 10-CH_3).

$^{13}C\{^1H\}$ NMR (151 MHz, $CDCl_3$, 25 °C, numbering of C is given in Fig. S1 in the ESI†): δ 199.41 (s, CO-β), 185.00 (s, CO-β), 171.66 (s, COO), 163.70 (s, 1′-C), 132.34 (s, 3′- & 5′-C), 121.30 (s, 4′-C), 114.20 (s, 2′- & 6′-C), 85.05 (s, CH-β), 68.30 (s, 1-C), 31.90, 29.56, 29.56, 29.36, 29.32 (s, 4–8-C), 29.09 (s, 2-C), 27.50 (s, CH_3-β), 25.98 (s, 3-C), 22.69 (s, 9-C), 20.81 (s, CH_3-β), 14.13 (s, 10-C).

2.2.2 Synthesis of the Rh complex (1): 2,4-dioxo-3-pentyl-4-decanyloxybenzoate rhodium(I)-dicarbonyl, [Rh(β-L1)$(CO)_2$]. The β-diketone ligand Hβ-L1 (synthesised in 2.2.1) 2,4-dioxo-3-pentyl-4-decanyloxybenzoate (0.536 mmol, 0.14 g) and sodium acetate (0.536 mmol, 44.0 mg) were dissolved in a few drops of methanol. A saturated solution of rhodium dimer [$Rh_2(\mu$-Cl$)_2(CO)_4$] (Sigma Aldrich, 0.268 mmol, 104 mg) in

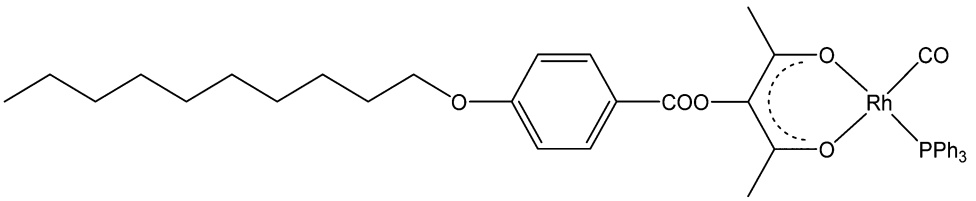

Fig. 2 Structure of the [Rh(β-L1)(CO)PPh_3] complex (**2**) of this study, with the β-diketonato ligand, β-L1, containing a long and sterically large α-substituent, $R^\alpha = C_{10}H_{21}OC_6H_4COO$.

methanol was slowly added into the β-diketone-sodium acetate solution. The vials were washed with more methanol, also adding the washings to the reaction mixture. Ice was added to force precipitation of a yellow-orange product and the reaction mixture was stirred for an hour at room temperature. The resulting precipitate was recrystallized from hexane, yielding the expected rhodium dicarbonyl complex (**1**), with a yield of 0.1029 g (74%).

^{1}H NMR (600 MHz, $CDCl_3$, 25 °C, numbering of C is given in Fig. S2 in the ESI†): δ 8.11 (d, $^{3}J_{H-H}$ = 8.9 Hz, 3′- & 5′-H), 6.96 (d, $^{3}J_{H-H}$ = 8.9 Hz, 2′- & 6′-H), 4.03 (t, $^{3}J_{H-H}$ = 6.6 Hz, 1-CH_2), 2.07 (s, CH_3-β), 1.81 (m, 2-CH_2), 1.47 (m, 3-CH_2), 1.40–1.20 (m, 4–9-CH_2), 0.88 (t, $^{3}J_{H-H}$ = 6.9 Hz, 10-CH_3).

$^{13}C\{^{1}H\}$ NMR (151 MHz, $CDCl_3$, 25 °C, numbering of C is given in Fig. S2 in the ESI†): δ 183.45 (d, $^{1}J_{Rh-C}$ = 73.2, CO), 182.52 (s, CO-β), 165.22 (s, COO), 163.78 (s, 1′-C), 132.28 (s, 3′- & 5′-C), 129.39 (s, CH-β), 120.98 (s, 4′-C), 114.45 (s, 2′- & 6′-C), 68.39 (s, 1-C), 31.89, 29.55, 29.55, 29.34, 29.31 (s, 4–8-C), 29.07 (s, 2-C), 25.97 (s, 3-C), 23.48 (s, CH_3-β), 22.68 (s, 9-C), 14.11 (s, 10-C).

IR peaks: 2079; 2005 ν(CO)/cm^{-1}.

2.2.3 Synthesis of the Rh complex (2): 2,4-dioxo-3-pentyl-4-decanyloxybenzoate-carbonyl-triphenyl-phosphine rhodium(I) (rhodium(triphenylphosphine)carbonyl-2,4-dioxo-3-pentyl-4-decanyloxybenzoate), [Rh(β-L1)(CO)(PPh_3)]. The synthesis was conducted according to published methods,[4,26,27] with slight changes. To a solution of the rhodium dicarbonyl complex (**1**), synthesised in 2.2.2, namely [Rh(β-L1)$(CO)_2$] (0.1 mmol, 0.0544 g) in 30 ml *n*-hexane, was added a solution of PPh_3 (0.1 mmol, 0.0262 g) in warm 15 ml *n*-hexane, which resulted in CO gas bubbling off. The resulting reaction mixture was stirred for 5 min in a boiling water bath, until no more CO gas was released and subsequently filtered while still warm. Pure crystals of the desired rhodium triphenylphosphine complex (**2**) were obtained by slowly cooling the filtered reaction mixture overnight at room temperature. Yield 0.0429 g (79.8%).

^{1}H NMR (600 MHz, $CDCl_3$, 25 °C, numbering of C is given in Fig. S3 in the ESI†): δ 8.09 (d, $^{3}J_{H-H}$ = 8.9 Hz, 3′- & 5′-H), 7.68 (m, b- & f-H), 7.44 (m, d-H), 7.40 (m, c- & e-H), 6.93 (d, $^{3}J_{H-H}$ = 8.9 Hz, 2′- & 6′-H), 4.02 (t, $^{3}J_{H-H}$ = 6.6 Hz, 1-CH_2), 2.10 (s, CH_3-β), 1.80 (m, 2-CH_2), 1.59 (s, CH_3-β), 1.46 (m, 3-CH_2), 1.40–1.20 (m, 4–9-CH_2), 0.88 (t, $^{3}J_{H-H}$ = 6.9 Hz, 10-CH_3).

$^{13}C\{^{1}H\}$ NMR (151 MHz, $CDCl_3$, 25 °C, numbering of C is given in Fig. S3 in the ESI†): δ 189.01 (d, $^{1}J_{Rh-C}$ = 76.2 Hz, $^{2}J_{P-C}$ = 25.2 Hz, CO), 182.56 (s, CO-β), 180.05 (s, CO-β), 165.55 (s, COO), 163.48 (s, 1′-C), 134.51 (d, $^{2}J_{P-C}$ = 11.5 Hz, b- & f-C), 132.14 (s, 3′- & 5′-C), 130.35 (s, d-C), 129.25 (s, C-β), 128.52 (d, $^{1}J_{P-C}$ = 12.1 Hz, a-C), 128.08 (d, $^{3}J_{P-C}$ = 10.9 Hz, c- & e-C), 121.57 (s, 4′-C), 114.28 (s, 2′- & 6′-C), 68.31 (s, 1-C), 31.89, 29.55, 29.55, 29.34, 29.32 (s, 4–8-C), 29.07 (s, 2-C), 25.97 (s, 3-C), 24.06 (s, CH_3-β), 23.13 (s, CH_3-β), 22.69 (s, 9-C), 14.13 (s, 10-C).

$^{31}P\{^{1}H\}$ NMR (243 MHz, $CDCl_3$, 25 °C): δ 49.24 (d, $^{1}J_{Rh-P}$ = 176.4 Hz).

IR peaks: 1983 ν(CO)/cm^{-1}.

2.3 Spectroscopy and spectrophotometry

The ^{1}H, ^{13}C and ^{31}P NMR spectra of all the products were recorded at 600.28, 150.96 and 242.99 MHz respectively, on a 600 MHz Bruker AVANCE II spectrometer, at 25 °C. All the samples were dissolved in deuterated chloroform. The chemical shifts were reported relative to $SiMe_4$ (0.00 ppm) for the ^{1}H and ^{13}C spectra, and relative to 85% H_3PO_4 (0 ppm) for the ^{31}P spectra. Positive values indicate a downfield shift. FTIR measurements (solid samples) were determined by a Bruker Tensor 27 IR spectrometer and Pike MIRacle ATR, running OPUS software (Version 1.1). Infrared spectra in solution were recorded on a Bruker Tensor 27 infrared spectrometer. UV measurements were recorded on a Shimadzu UV-1650PC UV/vis spectrometer, equipped with a multi-cell thermostated cell holder (±0.1 °C).

2.4 Kinetic measurements

Oxidative addition reactions were monitored by spectrophotometry, namely by IR (monitoring formation and disappearance of the carbonyl peaks), by UV/vis (monitoring the change in absorbance at wavelength 334 nm, in chloroform), and by ^{1}H and ^{31}P-NMR spectroscopy (by monitoring the change in integration units of the various signals with time). All kinetic measurements were monitored under pseudo first order conditions (varying the concentration of one reactant while keeping the other constant, by being in excess), with the concentration of [CH_3I] at 10 to 1000 times the concentration of the [Rh(β-L1)(CO)PPh_3] complex in the specified solution (therefore staying basically constant relative to the complex). The concentration of complex (**2**) was in the order of [Rh(β-L1)(CO)PPh_3] = 0.00005 mol dm^{-3} for UV/vis measurements and = 0.001 mol dm^{-3} for IR measurements. Kinetic measurements, under pseudo first order conditions, for different concentrations of [Rh(β-L1)(CO)PPh_3] at a constant [CH_3I] concentration, confirmed that the concentration of complex (**2**) [Rh(β-L1)(CO)PPh_3] did not influence the value of the observed kinetic rate constant. The observed first order rate constants (k_{obs}) were obtained from least-square fits of absorbance *vs.* time data.[28] The [Rh(β-L1)(CO)PPh_3] complex (**2**) was tested for stability for at least 24 hours, by NMR in a deuterated chloroform solution.

2.5 Calculations

Pseudo first order rate constants, k_{obs}, were calculated by fitting[28] the experimentally obtained kinetic data to the first order equation:[29]

$$A_t - A_\infty = (A_0 - A_\infty)e^{(-k_{obs} \times t)} \quad (1)$$

with A_t, A_∞ and A_0 being the absorbance of the indicated species at time t, infinity and at time 0 respectively. The experimentally determined pseudo first order rate constants (k_{obs}) were converted to the second order rate constants, k_1 (in dm^3 mol^{-1} s^{-1}), by determining the slope of the linear plots of k_{obs} against the concentration of the incoming iodomethane ligand. Non-zero intercepts implied that:

$$k_{obs} = k_1[CH_3I] + k_{-1}, \quad (2)$$

with k_1 = second order rate constant of the forward reaction of the first kinetic step (Scheme 4) and k_{-1} = first order rate

Table 1 Kinetic rate constants (k_1, k_2 and k_3) for the oxidative addition of iodomethane to [Rh(Hβ-L1)(CO)(PPh_3)], complex (**2**), in chloroform at 25 °C, as monitored by IR, NMR and UV/vis

	T	Rh(I) depletion	Rh(III)-alkyl1 formation	Rh(III)-acyl1 formation	Rh(III)-alkyl1 depletion	Rh(III)-acyl1 depletion	Rh(III)-alkyl2 formation
	°C	k_1/mol^{-1} dm^3 s^{-1}	k_1/mol^{-1} dm^3 s^{-1}	k_1/mol^{-1} dm^3 s^{-1}	k_2/s^{-1}	k_2/s^{-1}	k_3/s^{-1}
IR	25	0.0200(1)	0.034(2)	0.019(1)	0.000054(6)	0.000101(2)	0.000080(1)
NMR	25				0.000050(2)	0.000040(3)	0.000056(2)
						0.000040(2)	
Activation parameters					$\Delta H^{\#}$/kJ mol^{-1}	$\Delta S^{\#}$/J mol^{-1}	$\Delta G^{\#}$/kJ mol^{-1} at 25 °C
UV/vis	15	0.0074(6)					
	25	0.0202(7)			55.9(7.84)	−90.8(26.3)	83.0
	35	0.0361(7)					

constant of backward reaction of the first kinetic step (Scheme 4). All kinetic mathematical fits were done utilizing the fitting program, Scientist version 3.0.[28] The error of all data is presented according to crystallographic conventions: for example in Table 1, the value obtained for k_1 = 0.034(2) dm^3 mol^{-1} s^{-1} implies that k_1 = (0.034 ± 0.002) dm^3 mol^{-1} s^{-1}. The activation parameters were determined from the Eyring relationship,[29] as shown in Fig. 6:

$$\ln\frac{k_1}{T} - \frac{\Delta H^{\#}}{RT} + \frac{\Delta S^{\#}}{R} + \ln\frac{k_B}{h} \quad (3)$$

with $\Delta H^{\#}$ = activation enthalpy, $\Delta S^{\#}$ = activation entropy, T = temperature, k_1 = second order rate constant of the first kinetic step (Scheme 4) at T, k_B = Boltzmann's constant, h = Planck's constant, R = universal gas constant.

2.6 Cyclic voltammetry

Cyclic voltammetry (CV) measurements were conducted on solutions of 0.5 mmol dm^{-3} compound, in dry oxygen-free acetonitrile, containing 0.1 mol dm^{-3} tetrabutylammonium hexafluorophosphate, ([N(^{n}Bu$_4$)][PF_6]) (Fluka electrochemical grade), as supporting electrolyte, under a blanket of purified argon at 25 °C, utilizing a Princeton Applied Research Parstat 2273 advanced electrochemical system. A three-electrode cell, consisting of a Pt auxiliary electrode, a glassy carbon working electrode (surface area 3.14 mm^2) and a Ag-wire pseudo reference electrode were used. The working electrode was polished on a Buhler polishing mat, first with a 1 micron and then with a $\frac{1}{4}$ micron diamond paste respectively. All cited potentials were referenced against the FcH/FcH$^+$ couple, as suggested by IUPAC.[30]

3 Results and discussion

3.1 Synthesis

To synthesize a β-diketone ligand containing a long chain on the α-position (Fig. 1), the R^{α} = 4-decyloxybenzoate ($C_{10}H_{21}OC_6H_4COOH$) which will act as the α-chain, dissolved in tetrahydrofuran (THF), was added drop-wise to a stirred suspension of sodium hydride (NaH) in THF, in order to deprotonate 4-decyloxybenzoate. Dimethylformamide (DMF) was added to the product, followed by the addition of 3-chloropentane-2,4-dione. The Cl^- atom of the latter compound was substituted by the $(C_{10}H_{21}OC_6H_4COO)^-$ chain, forming the required α-substituted β-diketone, namely ligand 2,4-dioxo-3-pentyl-4-decanyloxybenzoate ($CH_3COCH(C_{10}H_{21}OC_6H_4COO)COCH_3$), called ligand Hβ-L1 in this study; see Scheme 1. Only the enol form of ligand Hβ-L1 was observed by NMR. Enol (>85% at 298 K[31,32]) is often the dominant tautomer observed for 1,3-substituted β-diketones, containing aromatic and/or aliphatic side groups.

The rhodium dicarbonyl complex (**1**), [Rh(β-L1)$(CO)_2$], was synthesised by dissolving sodium acetate in methanol (to extract the enol H) and adding an equivalent amount of ligand Hβ-L1 (2,4-dioxo-3-pentyl-4-decanyloxybenzoate) into this sodium acetate solution. Half of this equivalent amount of the rhodium dimer [$Rh_2Cl_2(CO)_4$] was added, then stirred and the yellow product (**1**) precipitated; see Scheme 2. The characteristic symmetric and anti-symmetric stretching frequencies of the two CO-groups, obtained by infrared spectroscopy at 2079 and 2005 cm^{-1} respectively, confirmed complexation to rhodium.

The rhodium triphenylphosphine complex (**2**), [Rh(β-L1)(CO)-(PPh_3)], was synthesized by adapting published methods.[4,26] The rhodium dicarbonyl complex (**1**) [Rh(β-L1)$(CO)_2$] was dissolved in hot hexane, triphenylphosphine (PPh_3) was also added to the hot hexane, and the reaction mixture was stirred for thirty minutes in a water bath, until all the CO gas had bubbled off from the hot mixture; see Scheme 3. Upon cooling, a light yellow product (**2**) precipitated out. On the ^{31}P NMR spectrum, a doublet was observed at 49.24 ppm, due to coupling of phosphorous to the rhodium in [Rh(β-L1)(CO)(PPh_3)]. On the ^{1}H NMR spectrum, multiplet resonances were observed at *ca.* 6.3 ppm to 8.1 ppm, representing protons of the three phenyl groups of triphenylphosphine, as well as protons of the phenyl group of the long α-substituent $(C_{10}H_{21}OC_6H_4COO)^-$.

3.2 Kinetics

The [Rh(β-L1)(CO)PPh_3] + CH_3I oxidative addition reaction for complex (**2**) of this study (Fig. 2), was studied by NMR spectroscopy, IR and UV/vis spectrophotometry. The results are tabulated in Table 1, and visualized in Fig. 3 and 4 (IR results), Fig. S4 (ESI†) and Fig. 5 (NMR results) and Fig. 6 (UV/vis results). The IR and NMR studies gave information on the type of Rh^{III} (alkyl or acyl) reaction product(s), while the UV/vis study

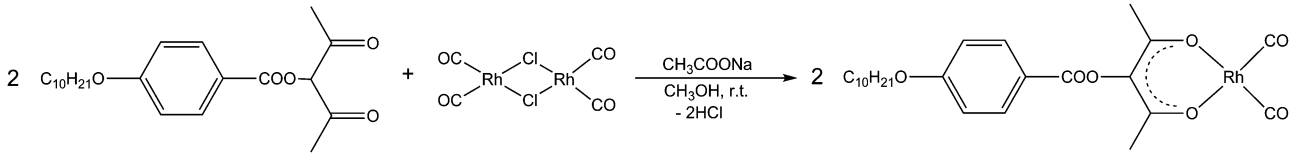

Scheme 2 Synthetic route for the synthesis of the rhodium dicarbonyl complex (**1**), [Rh(β-L1)(CO)$_2$], from ligand Hβ-L1 = $CH_3COCH(C_{10}H_{21}OC_6H_4COO)COCH_3$ (from Scheme 1).

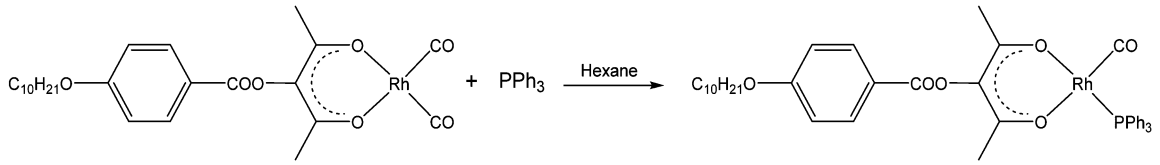

Scheme 3 Synthetic route for the synthesis of the rhodium triphenylphosphine complex (**2**), [Rh(β-L1)(CO)(PPh$_3$)], from complex (**1**) [Rh(β-L1)(CO)$_2$], (from Scheme 2), containing ligand Hβ-L1 = $CH_3COCH(C_{10}H_{21}OC_6H_4COO)COCH_3$.

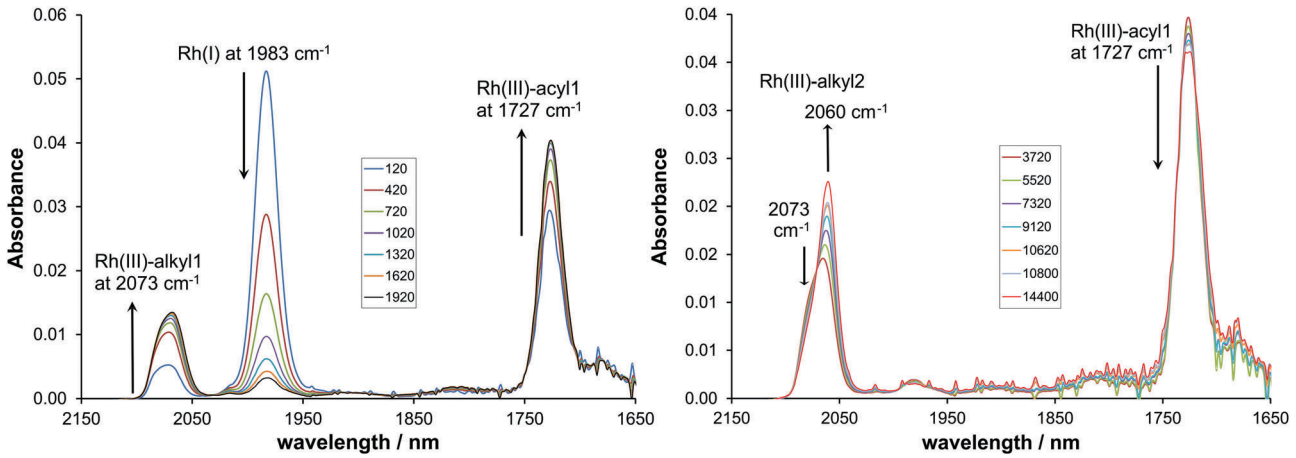

Fig. 3 Selected IR spectra, demonstrating the disappearance and appearance of the different reactants and products respectively, recorded at the indicated times in seconds (shown in various colours on the graph), during the IR monitoring of the reaction of complex (**2**), [Rh(β-L1)(CO)PPh$_3$] + CH_3I, in chloroform. Left: Reaction step 1, with k_{obs} (Rh^I disappearance) = 0.002 s^{-1} (k_1 = 0.02 mol^{-1} dm^3 s^{-1} in Scheme 4). Right: Reaction step 2, with k_{obs} (Rh^{III}-alkyl2 appearance) = 0.000080(1) s^{-1} (k_3 in Scheme 4). Initial concentrations were [Rh(β-L1)(CO)PPh$_3$] = 0.001 M, [CH_3I] = 0.1 M.

provided reaction rates at different temperatures, in order to calculate activation parameters. The proposed reaction scheme is given in Scheme 4.

3.2.1 IR study. Infrared spectrophotometry is useful for monitoring the disappearance and appearance of carbonyl peaks during the oxidative addition reaction of complex (**2**), due to the difference in stretching frequency, ν(CO), in the reactants or products of the reaction: the CO bonds in the various rhodium(I) complexes, [Rh^I(β-diketonato)(CO)(PPh$_3$)], resonate at a stretching frequency, ν(CO), of *ca.* 1970–1984 cm^{-1} (see Table 2, also for related complexes from literature), while shifting to a higher value of *ca.* 2050–2100 cm^{-1} for the oxidised [Rh^{III}(β-diketonato)(CH_3)(I)(CO)PPh$_3$] (Rh^{III}-alkyl) complexes. On the other hand, the CO bonds in the [Rh^{III}(β-diketonato)-($COCH_3$)(I)PPh$_3$] (Rh^{III}-acyl) complexes resonate at a much lower stretching frequency of *ca.* 1700–1750 cm^{-1}.[27] These distinctly different values of stretching frequencies ν(CO) for the Rh^I, Rh^{III}-alkyl and Rh^{III}-acyl complexes, enable distinction by IR between the Rh^I reactant and the different Rh^{III} products of the [Rh(β-L1)(CO)PPh$_3$] + CH_3I oxidative addition reaction of this study. Two reaction steps could be identified from the IR monitoring of this [Rh(β-L1)(CO)PPh$_3$] + CH_3I reaction in chloroform, as illustrated by the two graphs in Fig. 3, and formulated in Scheme 4. The first step involves the disappearance of the Rh^I in complex (**2**), as the CH_3I oxidatively adds to Rh^I, forming a Rh^{III}-alkyl1 intermediate product. However, the Rh^{III}-alkyl1 product seems to be in fast equilibrium with the Rh^{III}-acyl1 product of CO insertion, since the rate of formation of both Rh^{III}-alkyl1 and Rh^{III}-acyl1 is in the same order as the rate of depletion of Rh^I, namely $k_1 \approx 0.02$ mol^{-1} dm^3 s^{-1}; see Table 1. (The rate of formation of the Rh^{III}-alkyl1 species at 2073 cm^{-1}, $k_1 \approx 0.03$ mol^{-1} dm^3 s^{-1}, is virtually only slightly higher than the rate of disappearance of Rh^I, due to the fact that the intermediate Rh^{III}-alkyl1 is simultaneously being converted to Rh^{III}-acyl1 at 1727 cm^{-1}). During the second reaction step, both Rh^{III}-alkyl1 and Rh^{III}-acyl1 disappear at roughly the

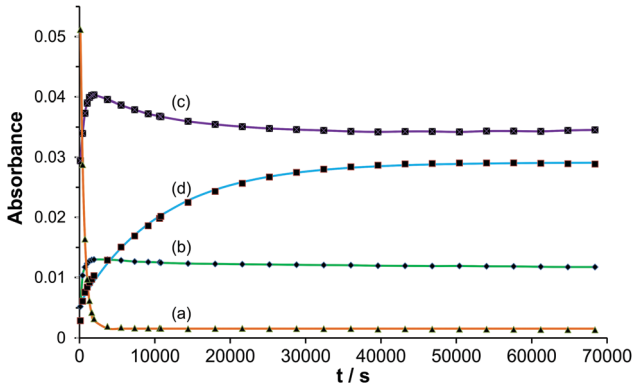

Fig. 4 Relative absorbance *vs.* time data of the different reactants and products, during the IR monitoring of the oxidative addition reaction of complex (**2**), [Rh(β-L1)(CO)PPh$_3$] + CH$_3$I: (a) Rh(I) depletion measured at 1983 cm^{-1}, (b) Rh(III)-alkyl1 formation and depletion measured at 2073 cm^{-1}, (c) Rh(III)-acyl1 formation and depletion measured at 1727 cm^{-1} and (d) Rh(III)-alkyl2 formation and depletion measured at 2060 cm^{-1}. Initial concentrations were [Rh(β-L1)(CO)PPh$_3$] = 0.001 M and [CH$_3$I] = 0.1 M.

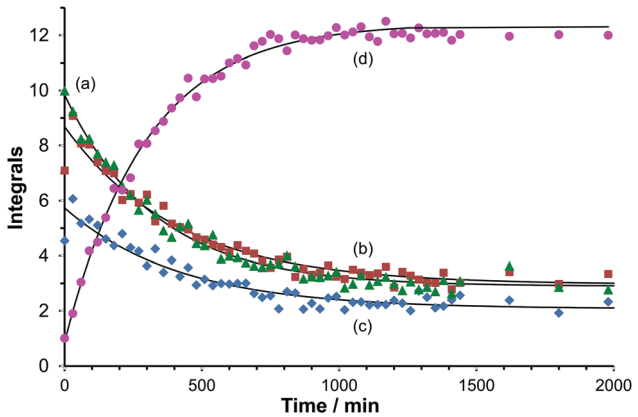

Fig. 5 Relative integration units *vs.* time data of the different reactants and products, during the ^{31}P NMR monitoring of the reaction of complex (**2**), [Rh(β-L1)(CO)PPh$_3$] + CH$_3$I: (a) Rh(III)-alkyl1 depletion, (b) and (c) Rh(III)-acyl1 and Rh(III)-acyl1′ depletion and (d) Rh(III)-alkyl2 formation.

same rate of *ca.* 0.00005 s^{-1} (see Table 1), as the new Rh^{III}-alkyl2 product is being formed. After 70 000 s (19 hours), virtually no initial Rh^{I} remained in the reaction solution, while an equilibrium was obtained between the three Rh^{III} reaction products present in the reaction solution, namely Rh^{III}-alkyl1, Rh^{III}-acyl1 and Rh^{III}-alkyl2, see Fig. 4. The absorbance is not related to the concentration of the different reaction products, therefore the IR data cannot provide the relative amounts of the reaction products in the solution.

3.2.2 NMR study. The reaction between iodomethane and the rhodium(I) complex (**2**) of this study was also monitored by ^{31}P NMR. The phosphorous peak of the rhodium-PPh$_3$ complex is a doublet, due to coupling between phosphorous (spin 1/2) and rhodium (spin 1/2). The ^{31}P doublet of the different [Rh^{I}(β-diketonato)(CO)(PPh$_3$)], Rh^{III}-alkyl and Rh^{III}-acyl reaction products, can conveniently be distinguished by the values of the $^{1}J(^{31}\text{P}–^{103}\text{Rh})$ coupling, namely *ca.* 170 ppm for Rh^{I} complexes, *ca.* 120 ppm for Rh^{III}-alkyl complexes and *ca.* 150 ppm for Rh^{III}-acyl complexes.[16,18,21] Selected fragments of the ^{31}P NMR spectra, recorded during the oxidative addition of complex (**2**), [Rh^{I}(β-L1)(CO)(PPh$_3$)] + CH$_3$I in CDCl$_3$, are shown in Fig. S4 of the ESI.† The same two reaction steps observed by IR, shown in Scheme 4, were observed when following the reaction by ^{31}P NMR, although the first step was too fast to be followed kinetically by ^{31}P NMR. Some new information was obtained by ^{31}P NMR, namely that actually two Rh^{III}-acyl1 structural isomers exist in equilibrium with Rh^{III}-alkyl1. The acyl isomers are Rh^{III}-acyl1 at 38.54 ppm with $^{1}J_{\text{Rh–P}}$ = 153.1 Hz, as well as Rh^{III}-acyl1′ at 37.54 ppm with $^{1}J_{\text{Rh–P}}$ = 155.1 Hz. Thus, during the second reaction step, the Rh^{III}-alkyl1 at 34.63 ppm ($^{1}J_{\text{Rh–P}}$ = 124.0 Hz), as well as isomers Rh^{III}-acyl1 and Rh^{III}-acyl1′, all deplete at roughly the same rate as the rate of formation of the final Rh^{III}-alkyl2 product, at 31.15 ppm ($^{1}J_{\text{Rh–P}}$ = 118.1 Hz). After 4000 min (67 hours) no initial Rh^{I} was observed any longer, but the four Rh^{III} reaction products were observed in the reaction solution in equilibrium with each other, namely 16.4% Rh^{III}-alkyl1, 10.8% Rh^{III}-acyl1, 16.3% Rh^{III}-acyl1′ and 56.5% Rh^{III}-alkyl2. The NMR data thus proves that Rh^{III}-alkyl2 is in fact the main product (at 56.5%); see Fig. 5 for kinetic data measured until 2000 min (33 h).

3.2.3 UV/vis study. Results for the oxidative addition reaction of complex (**2**), [Rh^{I}(β-L1)(CO)(PPh$_3$)] + CH$_3$I, studied here by UV/vis spectrophotometry, are shown in Fig. 6 and listed in Table 1. The change in absorbance when rhodium(I) is converted to rhodium(III), was monitored at wavelength 334 nm. The second order rate constant, k_1 = 0.0202(7) dm^3 mol^{-1} s^{-1}, obtained for the first reaction step at 25 °C, is the same as obtained by the IR study at 25 °C.

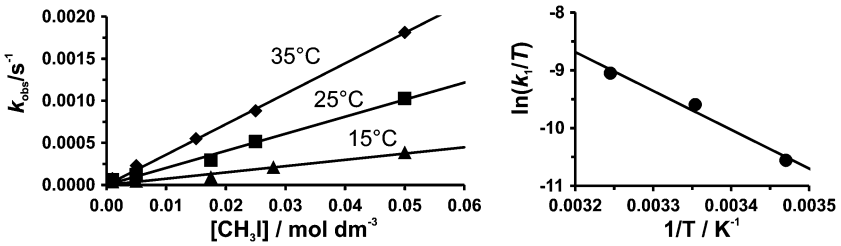

Fig. 6 Left: Temperature and [CH$_3$I] dependence of the pseudo first order rate constant (k_{obs}) for the first step of the oxidative addition reaction of complex (**2**), [Rh(β-L1)(CO)PPh$_3$] + CH$_3$I, in chloroform. λ(UV/vis) = 334 nm. (Temperatures: ▲ = 15 °C, ■ = 25 °C, ♦ = 35 °C.) Right: Eyring plot, giving the relation between k_1 and T, according to eqn (3).

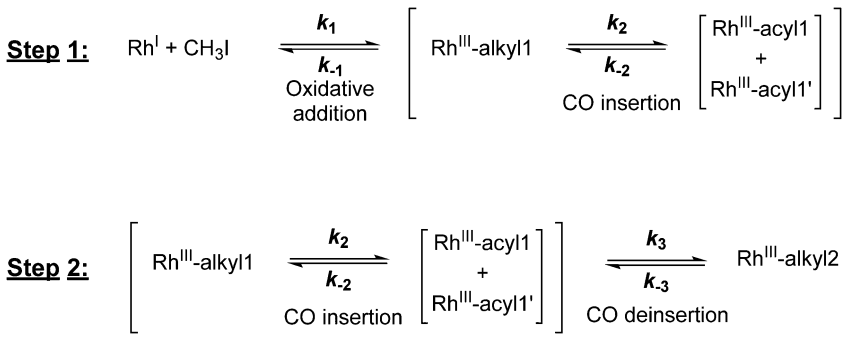

Scheme 4 The two reaction steps identified during the oxidative addition reaction of complex (**2**), [Rh(β-L1)(CO)PPh_3] + CH_3I.

The large negative activation entropy, $\Delta S^{\#} = -90(30)$ kJ K^{-1} mol^{-1}, is an indication towards associative activation during the transition state, while the positive activation enthalpy, $\Delta H^{\#} = 56(8)$ kJ mol^{-1}, shows that the oxidative addition reaction is endothermic, *i.e.* the products are more stable than the reactants. The transition state has an experimental energy barrier of $\Delta G^{\#}$ (298 K) = 83 kJ mol^{-1}. The experimental data supports an S_N2 mechanism for the [Rh^I(β-L1)(CO)(PPh_3)] + CH_3I oxidative addition reaction. This type of reaction is commonly proposed for addition of alkyl halides to square planar d^8 complexes, such as the Monsanto catalyst and other planar rhodium(I) complexes.[33–36] The S_N2 mechanism involves the nucleophilic attack by the d^8 rhodium(I) of [Rh^I(β-L1)(CO)(PPh_3)], complex (**2**), on the carbon of CH_3I, with the consequent formation of a polar, five-coordinated transitional state.[37] Addition of iodide in a fast follow-up step, leads to the formation of a [Rh^{III}(β-L1)(CH_3)(I)(CO)PPh_3] (Rh^{III}-alkyl1) product, see Scheme 5 for the proposed mechanism.

X-ray structures of the Rh^{III}-alkyl and Rh^{III}-acyl products, with iodide coordinated to rhodium, support the proposed mechanism in Scheme 5. For example, the Rh^{III}-alkyl products of the type [Rh(L,L′-BID)(CH_3)(I)(CO)PPh_3], where the iodide is coordinated to rhodium, have previously been isolated and characterized by solid state X-ray crystallography.[38–42] In this study, ligand L,L′-BID is a monocharged bidentate ligand, with donor atoms L and L′ (when L,L′ = O,O, then ligand L,L′-BID = β-diketonato ligand). Additionally, the Rh^{III}-acyl products of methyl migration, namely [Rh(L,L′-BID)($COCH_3$)(I)PPh_3], also with the iodide coordinated to rhodium, have been isolated and characterized by solid state X-ray crystallography.[43–45]

3.2.4 Reactivity correlation of the rate of iodomethane oxidative addition to a wide variety of different [Rh(β-diketonato)(CO)(PPh_3)] complexes without α-substituents. A literature study was conducted to obtain the IR (ν_{CO}), electrochemical (E_{pa}) and kinetic data (k_1) of the first oxidative addition step of the [Rh(β-diketonato)(CO)(PPh_3)] + CH_3I oxidative addition reaction, for a wide variety of 16 different β-diketonato ligands without α-substituents; see Table 2 for a summary of the data and the respective literature references. The ligand β-diketonato = $R^1COCR^{\alpha}COR^2$, with R^{α} = H in each example, except in ligand Hβ-L1 from this study, where group R^{α} = $C_{10}H_{21}OC_6H_4COO$ is a large and long chain. R^1 and R^2 on the β-diketonato ligand, are different combinations of substituents Fc (ferrocenyl), Ph (phenyl), Th (thienyl), CF_3 and alkyl $(CH_2)_nCH_3$, where n = 1–3.

Table 2 IR (ν_{CO}), electrochemical (E_{pa}) and kinetic data (k_1) as obtained from literature, for the oxidative addition reaction of a wide variety of [Rh(β-diketonato)(CO)(PPh_3)] complexes with CH_3I. β-diketonato ligand = $(R^1COCR^{\alpha}COR^2)^-$ (with R^{α} = H in each ligand below, except in the last ligand H(β-L1) from this study, where R^{α} = $C_{10}H_{21}OC_6H_4COO$)

Complex, with abbreviation for β-diketonato ligand	R^1	R^2	ν_{CO}/cm^{-1}	E_{pa}(Rh)/V *vs.* FcH/FcH^+	k_1/mol^{-1} dm^3 s^{-1}	Solvent kinetic	Ref. for k_1	Ref. for E_{pa}(Rh)
[Rh(dfcm)(CO)(PPh_3)]	Fc	Fc	1977	0.108	0.157(2)	Chloroform	19	46
[Rh(bab)(CO)(PPh_3)]	C_6H_5	$CH_2CH_2CH_3$	1981	—	0.0437(1)	Chloroform	22	—
[Rh(bfcm)(CO)(PPh_3)]	Fc	C_6H_5	1977	0.123	0.077(2)	Chloroform	19	46
[Rh(bap)(CO)(PPh_3)]	C_6H_5	CH_2CH_3	1982	—	0.0333(9)	Chloroform	22	—
[Rh(bav)(CO)(PPh_3)]	C_6H_5	$CH_2CH_2CH_2CH_3$	1983	—	0.0354(8)	Chloroform	22	—
[Rh(dtm)(CO)(PPh_3)]	C_4H_3S	C_4H_3S	1971	0.320	0.029(1)	Chloroform	18	49
[Rh(bth)(CO)(PPh_3)]	C_6H_5	C_4H_3S	1970	0.296	0.0265(6)	Chloroform	18	49
[Rh(acac)(CO)(PPh_3)]	CH_3	CH_3	1978	0.357	0.024(3)	1,2-Dichloroethane	15	49
[Rh(fca)(CO)(PPh_3)]	Fc	CH_3	1980	0.154	0.065(1)	Chloroform	19	46
[Rh(dbm)(CO)(PPh_3)]	C_6H_5	C_6H_5	1979	0.308	0.00961	Acetone	47	48
[Rh(ba)(CO)(PPh_3)]	C_6H_5	CH_3	1980	0.336	0.0093	Acetone	47	48
[Rh(fctfa)(CO)(PPh_3)]	Fc	CF_3	1986	—	0.00611(1)	Chloroform	17	46
[Rh(tta)(CO)(PPh_3)]	CF_3	C_4H_3S	1981	0.426	0.00171(4)	Chloroform	21	49
[Rh(tfaa)(CO)(PPh_3)]	CF_3	CH_3	1983	0.491	0.00146	Acetone	47	48
[Rh(tfba)(CO)(PPh_3)]	C_6H_5	CF_3	1983	0.448	0.00112	Acetone	47	48
[Rh(hfaa)(CO)(PPh_3)]	CF_3	CF_3	—	0.573	0.00013(1)	Chloroform	20	11
[Rh(β-L1)(CO)(PPh_3)]	CH_3	CH_3	1984	0.294	0.0202(7)	Chloroform	This study	This study

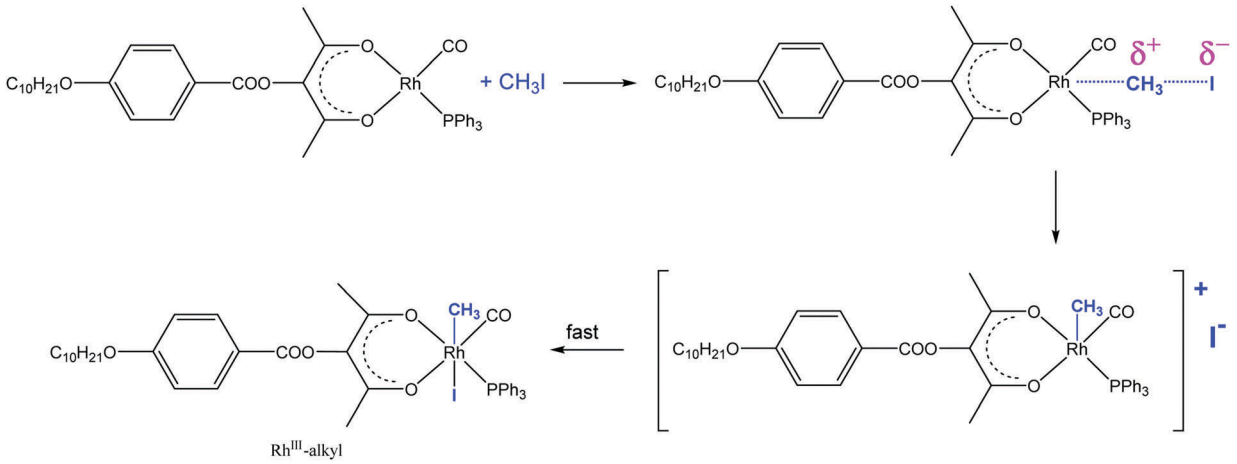

Scheme 5 Proposed S_N2 mechanism for the oxidative addition step of the reaction of complex (**2**), [Rh(β-L1)(CO)PPh$_3$] + CH_3I, with formation of the Rh^{III}-alkyl1 product.

All the second order rate constants (k_1) obtained for the first reaction step of the [Rh(β-diketonato)(CO)(PPh$_3$)] + CH_3I oxidative addition reaction, for this wide variety of 16 different β-diketonato ligands from literature, are summarized in Table 2 and visualized in Fig. 7. These [Rh(β-diketonato)(CO)(PPh$_3$)] complexes can clearly be divided into four groups: group 1 consists of those [Rh(β-diketonato)(CO)(PPh$_3$)] complexes with a β-diketonato ligand containing at least one electron donating Fc (ferrocenyl) group, with a larger value of $k_1 > 0.06$ dm^3 mol^{-1} s^{-1}. Group 2 are those [Rh(β-diketonato)(CO)(PPh$_3$)] complexes with a β-diketonato ligand containing only Ph, Th or alkyl groups, with k_1 values between $0.04 > k_1$ (dm^3 mol^{-1} s^{-1}) > 0.01. Group 3 are those [Rh(β-diketonato)(CO)(PPh$_3$)] complexes with a β-diketonato ligand containing one strongly electron withdrawing CF_3 group, with smaller values of $0.002 > k_1$ (dm^3 mol^{-1} s^{-1}) > 0.001. Group 4 consists of the [Rh(β-diketonato)(CO)(PPh$_3$)] complex with a β-diketonato ligand containing two strongly electron withdrawing CF_3 groups, with a much smaller value of $k_1 < 0.0001$ dm^3 mol^{-1} s^{-1}. The effect on the value of the second order oxidative addition rate constant k_1, when moving from group 4 to group 3 to group 2 to group 1, is roughly a tenfold increase in the value of k_1. The only complex whose k_1 value does not follow this trend, is complex [Rh(FcCOCHCOCF$_3$)(CO)PPh$_3$], which contains both an electron donating Fc group, as well as an electron withdrawing CF_3 group on the same ligand (= fctfa), causing it to neither fit into group 1 (with Fc substituents), nor

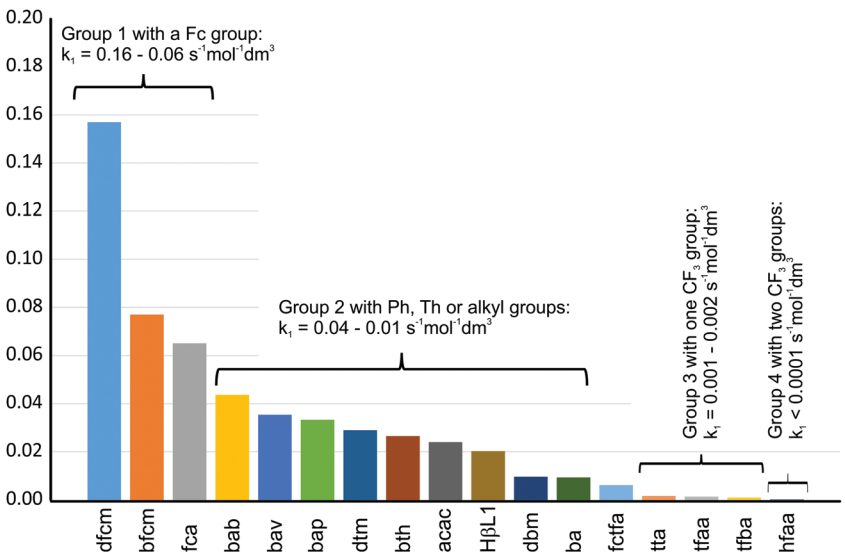

Fig. 7 Comparison of the second order rate constants k_1 (in mol^{-1} dm^3 s^{-1}) of the first oxidative addition step of the [Rh(β-diketonato)(CO)(PPh$_3$)] + CH_3I oxidative addition reaction, for a wide variety of different β-diketonato ligands without α-substituents, as obtained from literature, see Table 2. Ligand β-diketonato = $R^1COCR^\alpha COR^2$, with R^α = H in each example, except in ligand Hβ-L1 from this study, where group $R^\alpha = C_{10}H_{21}OC_6H_4COO$. R^1 and R^2 are different combinations of substituents Fc (ferrocenyl), Ph (phenyl), Th (thienyl), CF_3 and alkyl $(CH_2)_nCH_3$, where n = 1–3. Data is listed in Table 2. The complex with ligand fctfa fits neither into group 1 (with Fc substituents), nor into group 3 (with CF_3 substituents), since it contains both a Fc and CF_3 substituent.

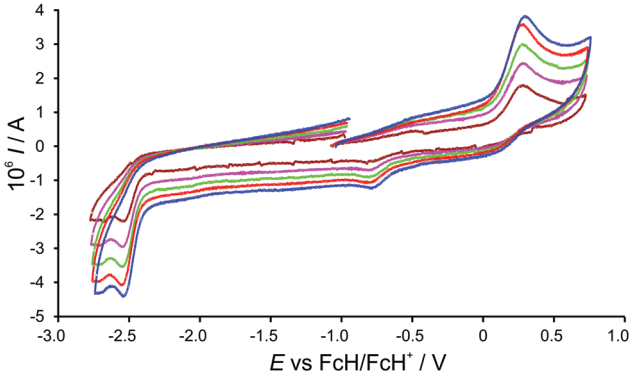

Fig. 8 Cyclic voltammograms of 0.0005 mol dm^{-3} solution of complex (**2**), [Rh(β-L1)(CO)(PPh$_3$)], at different scan rates of ν = 0.05 (brown, smallest peak currents), 0.10 (magenta), 0.15 (green), 0.20 (red) and 0.25 (blue, largest peak currents) V s^{-1}.

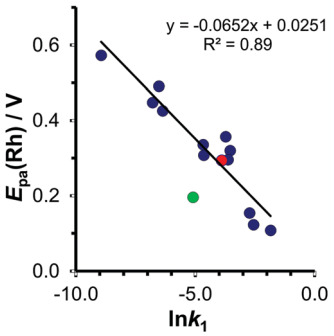

Fig. 9 Relationship between the second order rate constants k_1 (in mol^{-1} dm^3 s^{-1}) of the first oxidative addition step of complexes [Rh(β-diketonato)-(CO)(PPh$_3$)] with CH$_3$I, and the oxidation potential (E_{pa}) of the rhodium(I) metal in [Rh(β-diketonato)(CO)(PPh$_3$)], as obtained from literature for a wide variety of related Rh^{I} triphenylphosphine complexes with different ligands, see Table 2. Data of complex (**2**), [Rh(Hβ-L1)(CO)PPh$_3$], is indicated by the red dot and fits the general linear trend. The green dot indicates data of a specific complex [Rh(FcCOCHCOCF$_3$)(CO)PPh$_3$], which was not used in the linear fit (indicated by the black line), since it contains both electron donating (Fc) and electron withdrawing (CF$_3$) groups. Data is given in Table 2.

into group 3 (with CF$_3$ substituents), but to approximately fit into group 2.

3.3 Cyclic voltammetry

The cyclic voltammogram of complex (**2**), [Rh(β-L1)(CO)PPh$_3$], is shown in Fig. 8 at the indicated scan rates, with data summarized in Table 3. The oxidation of Rh^{I} to Rh^{III} is observed at 0.299 V, *versus* the FcH/FcH$^+$ couple. Reduction of a Rh^{III}-species is observed at −0.824 V, and the reduction of the coordinated β-L1 ligand is observed at −2.539 V (0.100 V s^{-1} values). The assignments of the redox processes are in accordance with published data for related [Rh(β-diketonato)(CO)(PPh$_3$)] complexes.[49] The electrochemical and chemical (obtained here by oxidative addition) oxidation of [Rh(β-diketonato)(CO)(PPh$_3$)], complex (**2**), both result in a Rh^{III} species. According to expectation, the potential at which the electrochemical oxidation of Rh^{I} occurs, relates to the rate constant k_1 (in dm^3 mol^{-1} s^{-1}) of the first step of the second order oxidative addition. This was found by comparing the E_{pa} and k_1 values of a series of 16 related Rh^{I} β-diketonato complexes from literature with complex (**2**) from this study (data summarized in Table 2). A linear correlation was found between E_{pa} and ln(k_1) of all the complexes; see Fig. 9. The trend observed here over a potential range of nearly 0.5 V, is, that with increasing difficulty to electrochemically oxidize rhodium(I) to rhodium(III) (indicated by higher E_{pa}(Rh) values), the kinetic rate of chemical oxidation (with CH$_3$I) also becomes increasingly slower. The data point of one specific complex with ligand fctfa, namely [Rh(FcCOCHCOCF$_3$)(CO)PPh$_3$], deviates slightly from the expected linear trend shown in Fig. 9, as indicated by the green data point. The reason for this deviation is (as also concluded from Fig. 7), since the fctfa ligand of this complex simultaneously contains a very electron donating substituent Fc, as well as a very electron withdrawing substituent CF$_3$, causing it to fit neither into group 1 (containing Fc) nor into group 3 (containing CF$_3$).

Table 3 Cyclic voltammetric data (the electrochemical oxidation and reduction potentials, E_{pa} and E_{pc}) obtained during the cyclic voltammetry analysis of complex (**2**) [Rh(β-L1)(CO)(PPh$_3$)], in 0.1 mol dm^{-3} [N(^{n}Bu$_4$)][PF$_6$]/CH$_3$CN, at the indicated scan rates (ν), at 25 °C

Compound	ν/V s^{-1}	E_{pa} (Rh)/V	E_{pc} (Rh)/V	E_{pc} (ligand)/V
[Rh(β-L1)(CO)(PPh$_3$)]	0.05	0.293	−0.798	−2.543
	0.10	0.294	−0.799	−2.547
	0.15	0.294	−0.799	−2.548
	0.20	0.295	−0.799	−2.549
	0.25	0.298	−0.800	−2.550

4 Conclusion

A new [Rh(β-diketonato)(CO)(PPh$_3$)] complex (**2**) was successfully synthesized and characterized, containing the β-diketonato ligand β-L1 = (CH$_3$COC(C$_{10}$H$_{21}$OC$_6$H$_4$COO)COCH$_3$)$^-$, with a long chain (C$_{10}$H$_{21}$OC$_6$H$_4$COO) at the α-position. The conversion of Rh^{I} to Rh^{III} of this complex was investigated both chemically (by IR, UV/vis and NMR) as well as electrochemically (by CV). The chemical conversion of Rh^{I} to Rh^{III} was obtained by oxidative addition of CH$_3$I to the Rh^{I}. Following the reaction kinetics of the [Rh(β-L1)(CO)PPh$_3$] + CH$_3$I reaction *via* IR spectra, demonstrated that this reaction occurs in two steps: the first reaction step is the disappearance of Rh^{I}, as the CH$_3$I oxidatively adds to Rh^{I} forming a Rh^{III}-alkyl1 product, which is in a fast equilibrium with a Rh^{III}-acyl1 product of CO insertion. During the second reaction step, the formation of a new Rh^{III}-alkyl2 main product was observed. Additionally, it was proven by NMR data obtained during the [Rh(β-L1)(CO)PPh$_3$] + CH$_3$I oxidative addition reaction, that actually two Rh^{III}-acyl1 structural isomers are present in the reaction solution of the first reaction step (Rh^{III}-acyl1 and Rh^{III}-acyl1′), forming the Rh^{III}-alkyl2 as the main reaction product during the second reaction step, at a percentage yield of 56.5%.

The reaction rate of the first oxidative addition step of [Rh(β-L1)(CO)PPh$_3$] + CH$_3$I in chloroform, k_1 = 0.0202(7) mol^{-1} dm^3 s^{-1}, was not at all influenced by the long and sterically

large chain ($C_{10}H_{21}OC_6H_4COO$) substituted at the α-position of the β-diketonato ligand, and is similar in value to the rate of oxidative addition (k_1) of related complexes without such long and steric substituents; for example the reaction of the similar complex $[Rh(CH_3COCHCOCH_3)(CO)(PPh_3)]$ + CH_3I, where k_1 = 0.024(3) mol^{-1} dm^3 s^{-1}, which is the same as k_1 for complex (**2**). The oxidation potential (E_{pa}) for the electrochemical oxidation of $[Rh^{I}(\beta\text{-L1})(CO)PPh_3]$ to Rh^{III} also is similar to that of related [Rh(β-diketonato)(CO)(PPh_3)] complexes without steric substituents. The oxidation potential of complex (**2**) fits into the linear extrapolation of the graph between the ln of the second order oxidative addition rate constant ($\ln k_1$) *versus* the oxidation potential E_{pa}(Rh), with a R^2 value of 0.89, proving that the chemical oxidation of $[Rh(\beta\text{-L1})(CO)PPh_3]$ also has not been influenced at all by the long chain ($C_{10}H_{21}OC_6H_4COO$) substituted at the α-position of the β-diketonato ligand, when compared to similar complexes from literature without an α-substituent.

Conflicts of interest

There are no conflicts to declare.

Acknowledgements

This work has received support from the South African National Research Foundation and the Central Research Fund of the University of the Free State, Bloemfontein, South Africa.

References

1 K. Binnemans, Rare-earth beta-diketonates, in *Handbook on the Physics and Chemistry of Rare Earths*, ed. K. A. Gschneidner (Jr.), J.-C. G. Bünzli and V. K. Pecharsky, Elsevier B.V., Amsterdam, North-Holland, 2005, ch. 225, vol. 35, DOI: 10.1016/S0168-1273(05)35003-3.

2 M. M. Conradie, A. J. Muller and J. Conradie, Thienyl-containing β-diketones: synthesis, characterization, crystal structure, keto–enol kinetics, *S. Afr. J. Chem.*, 2008, **61**, 13–21. http://www.journals.co.za/sajchem/.

3 J. Starý, *The Solvent Extraction of Metal Chelates*, MacMillan Company, New York, 1964.

4 F. Bonati and G. Wilkinson, Dicarbonyl-β-diketonato- and related complexes of rhodium(I), *J. Chem. Soc.*, 1964, 3156–3160, DOI: 10.1039/JR9640003156.

5 N. A. Bailey, E. Coates, G. B. Robertson, F. Bonati and R. Ugo, The Crystal and Molecular Structures of Acetylacetonatobiscarbonylrhodium(I) and of some Fluoro-substituted Complexes, *Chem. Commun.*, 1967, 1041–1042, DOI: 10.1039/C19670001041.

6 M. M. Conradie and J. Conradie, Solid state packing of [Rh(β-diketonato)$(CO)_2$] complexes. Crystal structure of $[Rh(PhCOCHCOC_4H_3S)(CO)_2]$, *J. Mol. Struct.*, 2013, **1051**, 137–143, DOI: 10.1016/j.molstruc.2013.07.046.

7 J. Conradie, A comparative DFT study of stacking interactions between adjacent metal atoms in linear chains of Ir and Rh acetylacetonato complexes, *J. Organomet. Chem.*, 2017, **833**, 88–94, DOI: 10.1016/j.jorganchem.2017.01.032.

8 K. H. Hopmann and J. Conradie, A Density Functional Theory Study of Substitution at the Square-Planar Acetylacetonato-dicarbonyl-rhodium(I) complex, *Organometallics*, 2009, **28**, 3710–3715, DOI: 10.1021/om900133s.

9 K. H. Hopmann, N. F. Stuurman, A. Muller and J. Conradie, Substitution and Isomerisation of Asymmetric β-Diketonato Rhodium(I) Complexes: A Crystallographic and Computational Study, *Organometallics*, 2010, **29**, 2446–2458, DOI: 10.1021/om1000138.

10 J. Conradie, Stacking of dicarbonylacetylacetonatorhodium(I) molecules, *Comput. Theor. Chem.*, 2017, **1101**, 30–35, DOI: 10.1016/j.comptc.2016.12.024.

11 J. Conradie, Density Functional Theory Calculations of Rh-β-diketonato complexes, *J. Chem. Soc., Dalton Trans.*, 2015, **44**, 1503–1515, DOI: 10.1039/C4DT02268H.

12 J. Conradie, Conformational analysis of triphenylphosphine in square planar organometallic complexes: $[(PPh_3)(ML_1L_2L_3)]$ and $[M(acac)(L')(PPh_3)]$, *J. Chem. Soc., Dalton Trans.*, 2012, **41**, 10633–10642, DOI: 10.1039/C2DT30850A.

13 M. M. Conradie and J. Conradie, Methyl Iodide Oxidative Addition to $[Rh(acac)(CO)(PPh_3)]$: an Experimental and Theoretical Study of the Stereochemistry of the Products and the Reaction Mechanism, *J. Chem. Soc., Dalton Trans.*, 2011, **40**, 8226–8237, DOI: 10.1039/c1dt10271k.

14 J. F. Roth, The Production of Acetic Acid: Rhodium Catalysed Carbonylation of Methanol, *Platinum Met. Rev.*, 1975, **19**, 12–14, DOI: 10.1.1.562.6829.

15 S. S. Basson, J. G. Leipoldt, A. Roodt, J. A. Venter and T. J. van der Walt, The oxidative addition of iodomethane to acetylacetonatocarbonylphosphinerhodium(I) complexes, *Inorg. Chim. Acta*, 1986, **119**, 35–38, DOI: 10.1016/S0020-1693(00)81327-4.

16 Y. S. Varshavsky, T. G. Cherkasova, N. A. Buzina and L. S. Bresler, Spectral characteristics of products formed by reaction between Rhacac(PPh_3)(CO) and methyl iodide, *J. Organomet. Chem.*, 1994, **464**, 239–245, DOI: 10.1016/0022-328X(94)87280-5.

17 J. Conradie, G. J. Lamprecht, A. Roodt and J. C. Swarts, Kinetic study of the oxidative addition reaction between methyl iodide and $[Rh(FcCOCHCOCF_3)(CO)(PPh)_3]$: Structure of $[Rh(FcCOCHCOCF_3)(CO)(PPh)_3(CH_3)(I)]$, *Polyhedron*, 2007, **23**, 5075–5087, DOI: 10.1016/j.poly.2007.07.004.

18 M. M. Conradie and J. Conradie, Methyl Iodide Oxidative Addition to Monocarbonylphosphine $[Rh((C_4H_3S)COCHCOR)(CO)(PPh_3)]$ Complexes, utilizing UV/vis and IR Spectrophotometry and NMR Spectroscopy to identify Reaction Intermediates. R = C_6H_5 or C_4H_3S, *Inorg. Chim. Acta*, 2008, **361**, 2285–2295, DOI: 10.1016/j.ica.2007.10.052.

19 J. Conradie and J. C. Swarts, Oxidative Addition of CH_3I and CO Migratory Insertion in a series of Ferrocene-containing Carbonyl Phosphine β-Diketonato Rhodium(I) Complexes, *Organometallics*, 2009, **28**, 1018–1026, DOI: 10.1021/om800655j.

20 S. S. Basson, J. G. Leipoldt and J. T. Nel, The oxidative addition of methyl iodide to β-diketonecarbonyltriphenylphosphinerhodium(I) complexes, *Inorg. Chim. Acta*, 1984, **84**, 167–172, DOI: 10.1016/S0020-1693(00)82403-2.

21 M. M. Conradie and J. Conradie, A Kinetic Study of the Oxidative Addition of Methyl Iodide to [Rh((C$_4$H$_3$S)-COCHCOCF$_3$)(CO)(PPh$_3$)] utilizing UV/vis and IR Spectrophotometry and ^{1}H, ^{19}F and ^{31}P NMR Spectroscopy. Synthesis of [Rh((C$_4$H$_3$S)COCHCOCF$_3$)(CO)(PPh$_3$)(CH$_3$)(I)], *Inorg. Chim. Acta*, 2008, **361**, 208–218, DOI: 10.1016/j.ica.2007.07.010.

22 N. F. Stuurman and J. Conradie, Iodomethane Oxidative Addition and CO Migratory Insertion in Monocarbonylphosphine Complexes of the type [Rh((C$_6$H$_5$)COCHCO-((CH$_2$)$_\eta$CH$_3$))(CO)(PPh$_3$)]: Steric and Electronic Effects, *J. Organomet. Chem.*, 2009, **694**, 259–268, DOI: 10.1016/j.jorganchem.2008.10.040.

23 V. Bocokić, A. Kalkan, M. Lutz, A. L. Spek, D. T. Gryko and J. N. H. Reek, Capsule-controlled selectivity of a rhodium hydroformylation catalyst, *Nat. Commun.*, 2013, **4**, 2670, DOI: 10.1038/ncomms3670.

24 R. Ugo, A. Pasini, A. Fusi and S. Cerini, Kinetic investigation of some electronic and steric factors in oxidative addition reactions to Vaska's compound, *J. Am. Chem. Soc.*, 1972, **94**, 7364–7370, DOI: 10.1021/ja00776a017.

25 B. S. Furniss, A. J. Hannaford, P. W. G. Smith and A. R. Tatchell, *Vogel's Textbook of Practical Organic Chemistry*, John Wiley & Sons, New York, 5th edn, 1994, p. 409.

26 (*a*) D. E. Graham, G. J. Lamprecht, I. M. Potgieter, A. Roodt and J. G. Leipoldt, *Transition Met. Chem.*, 1991, **16**, 193–199, DOI: 10.1007/BF01032832; (*b*) J. G. Leipoldt, S. S. Basson and J. T. Nel, The crystal structure of 1,1,1,-trifluoro-5,5-dimethylpentanedionato-carbonyltriphenylphosphinerhodium(I), *Inorg. Chim. Acta*, 1983, **74**, 85–88, DOI: 10.1016/S0020-1693(00)81410-3; (*c*) J. J. C. Erasmus and J. Conradie, Chemical and electrochemical oxidation of [Rh(β-diketonato)(CO)(P(OCH$_2$)$_3$CCH$_3$)]: an experimental and DFT study, *J. Chem. Soc., Dalton Trans.*, 2013, **42**, 8655–8666, DOI: 10.1039/C3DT50310K.

27 J. Conradie, G. J. Lamprecht, S. Otto and J. C. Swarts, Synthesis and characterisation of ferrocene-containing β-diketonato complexes of rhodium(I) and rhodium(III), *Inorg. Chim. Acta*, 2002, **328**, 191–203, DOI: 10.1016/S0020-1693(01)00731-9.

28 Scientist (©1993–2008) Version 3.0, MicroMath Software Inc., Saint Louis, Missouri, 63144.

29 J. H. Espenson, *Chemical Kinetics and Reaction Mechanisms*, McGraw-Hill, New York, 2nd edn, 1995, pp. 15, 49, 70–75, 156.

30 G. Gritzner and J. Kuta, Recommendations on reporting electrode potentials in nonaqueous solvents, *Pure Appl. Chem.*, 1984, **56**, 461–466, DOI: 10.1351/pac198456040461.

31 R. C. Mehrotra, R. Bohra and D. P. Gaur, *Metal β-diketonates and allied derivatives*, Academic Press, London, 1978.

32 J. L. Burdett and M. T. Rogers, Keto–Enol Tautomerism in β-Dicarbonyls Studied by Nuclear Magnetic Resonance Spectroscopy. I. Proton Chemical Shifts and Equilibrium Constants of Pure Compounds, *J. Am. Chem. Soc.*, 1964, **86**, 2105–2109, DOI: 10.1021/ja01065a003.

33 T. R. Griffin, D. B. Cook, A. Haynes, J. M. Pearson, D. Monti and G. E. Morris, Theoretical and Experimental Evidence for S_N2 Transition States in Oxidative Addition of Methyl Iodide to *cis*-[M(CO)$_2$I$_2$]$^-$ (M = Rh, Ir), *J. Am. Chem. Soc.*, 1996, **118**, 3029–3030, DOI: 10.1021/ja952952o.

34 P. M. Maitlis, A. Haynes, G. J. Sunley and M. J. Howard, Methanol carbonylation revisited: thirty years on, *J. Chem. Soc., Dalton Trans.*, 1996, 2187–2196, DOI: 10.1039/DT9960002187.

35 G. J. van Zyl, G. J. Lamprecht, J. G. Leipoldt and T. W. Swaddle, Kinetics and mechanism of the oxidative addition of iodomethane to β-diketonatobis(triphenylphosphite)rhodium(I) complexes, *Inorg. Chim. Acta*, 1988, **143**, 223–227, DOI: 10.1016/S0020-1693(00)83693-2.

36 M. M. Conradie and J. Conradie, A density functional theory study of the oxidative addition of methyl iodide to square planar [Rh(acac)(P(OPh)$_3$)$_2$] complex and simplified model systems, *J. Organomet. Chem.*, 2010, **695**, 2126–2133, DOI: 10.1016/j.jorganchem.2010.05.021.

37 F. A. Cotton and G. Wilkinson, *Basic Inorganic Chemistry*, John Wiley & Sons, New York, 1976, pp. 529–547.

38 K. G. van Aswegen, J. G. Leipoldt, I. M. Potgieter, G. J. Lamprecht, A. Roodt and G. J. van Zyl, The crystal structure of the acetone adduct of *trans*-methyliodo-8-hydroxyquinolinatocarbonyltriphenylphosphinerhodium(III), *Transition Met. Chem.*, 1991, **16**, 369–371, DOI: 10.1007/BF01024085.

39 P. Braunstein, Y. Chauvin, J. Fischer, H. Olivier, C. Strohmann and D. V. Toronto, Oxidative addition of iodine, iodomethane and iodobenzene to the rhodium phosphino enolate complex [Rh{Ph$_2$PCH=C(=O)Ph}(CO)(PPh$_3$)] and carbon monoxide insertion into the resulting Rh–carbon bond of [Rh{Ph$_2$PCH=C(=O)Ph}Me(I)(CO)(PPh$_3$)], *New J. Chem.*, 2000, **24**, 437–445, DOI: 10.1039/B000961J.

40 S. S. Basson, J. G. Leipoldt, A. Roodt and J. A. Venter, Mechanism for the oxidative addition of Iodomethane to carbonyl(*N*-hydroxy-*N*-nitrosobenzenaminato-*O*,*O*′)triarylphosphinerhodium(I) complexes and crystal structure of [Rh(cupf)(CO)(CH$_3$)(I)(PPh$_3$)], *Inorg. Chim. Acta*, 1987, **128**, 31–37, DOI: DOI:10.1016/S0020-1693(00)84691-5.

41 M. Cano, J. V. Heras, M. A. Lobo, E. Pinilla and M. A. Monge, Oxidative additions of I_2 and CH_3I to [Rh(quin)(CO)|P(R-C$_6$H$_4$)$_3$|] complexes. Crystal structure of [Rh(I)(CH$_3$)(quin)-(CO)|P(4-CH$_3$-C$_6$H$_4$)$_3$|]·12Et$_2$O—IV, *Polyhedron*, 1992, **11**, 2679–2690, DOI: 10.1016/S0277-5387(00)80239-9.

42 L. J. Damoense, W. Purcell, A. Roodt and J. G. Leipoldt, Crystal structure of (2-amino-vinyl-4-pentanonato-κO,κN)-carbonyltriphenylphosphine, *Rhodium Express*, 1994, **5**, 10–13.

43 J. A. Cabeza, V. Riera, M. A. Villa-García, L. Ouahab and S. Triki, Synthesis and reactivity of dithiodiphenylphosphinato-derivatives of rhodium. Crystal structure of the square-pyramidal rhodium(III) complex [RhI(η^2-S$_2$PPh$_2$)(COMe)(PPh$_3$)], *J. Organomet. Chem.*, 1992, **441**, 323–331, DOI: 10.1016/0022-328X(92)83391-T.

44 C.-H. Cheng, B. D. Spivack and R. Eisenberg, The addition of alkyl halides to rhodium(I) dithiolene complexes. The synthesis, structure, and chemical properties of rhodium(III) acyl species, *J. Am. Chem. Soc.*, 1977, **99**, 3003–3011, DOI: 10.1021/ja00451a025.

45 L. J. Damoense, W. Purcell and A. Roodt, Carbonyl Insertion in Rh(III) Complexes: Crystal Structure of Acyl(2-Iminopentan-4-onato-O,N)iodotriphenylphosphinerhodium(III), *Rhodium Express*, 1995, **14**, 4–9.

46 J. Conradie and J. C. Swarts, The Relationship Between the Electrochemical and Chemical Oxidation of Ferrocene-Containing Carbonyl Phosphine β-Diketonato Rhodium(I) Complexes; Cytotoxicity of [Rh(FcCOCHCOPh)(CO)(PPh_3)], *Eur. J. Inorg. Chem.*, 2011, 2439–2449, DOI: 10.1002/ejic.201100007.

47 D. Lamprecht, PhD thesis, University of the Orange Free State, R.S.A., 1998.

48 D. Lamprecht and G. J. Lamprecht, Electrochemical oxidation of Rh(I) to Rh(III) in rhodium(I) β-diketonato carbonyl phosphine complexes, *Inorg. Chim. Acta*, 2000, **309**, 72–76, DOI: 10.1016/S0020-1693(00)00235-8.

49 H. Ferreira, M. M. Conradie and J. Conradie, Electrochemical study of Carbonyl Phosphine β-Diketonato Rhodium(I) Complexes, *Electrochim. Acta*, 2013, **113**, 519–526, DOI: 10.1016/j.electacta.2013.09.099.

